Original Manuscript

Characterization of nanocomposite tetrahedral amorphous carbon coated drill bits for improved drilled-hole quality in carbon fiber-reinforced polymer/ Al7075-T6 stacks

Joy Mathavan Jebaratnam[1,2], Muhammad Hafiz Hassan[1,3] ⓘ, Abdus Samad Mahmud[1] and Franz Gérald[4]

Abstract

The use of hybrid composite stacks is kept on increasing in the aircraft industry due to their numerous advantages in this sector. Therefore, improving the drilled-hole quality is also sought over time. The present work focuses on the effect of metallic elements-doped tetrahedral amorphous carbon coated drill bits on the drilled-hole quality while performing single-shot drilling of CFRP/Al7075-T6 stacks. This was evaluated from CFRP exit delamination and Al7075-T6 exit burr height. Mechanical and tribological properties of three different tetrahedral amorphous carbon (ta-C) coating-types, i.e. micro-, chromium-doped (:Cr) and titanium-doped (:Ti) were compared to uncoated tool ones. Bonding strength of the selected coatings with the tool was also calculated. Process capability six pack analysis was used to validate the experimental results obtained for drilled-hole quality. It was shown that micro-ta-C coating-type exhibited maximum hardness. The hardness value directly influences the exit delamination. It was found that CFRP exit delamination decreased as the hardness of the drill bit increased. Moreover, the multi-material stacks drilled with ta-C:Cr coated tool presented the lowest burr height (less than 150 μm), compared to the other tested coating-types. Low-friction surfaces seem to promote low exit burr height.

Keywords

Hole edge analysis, carbon fiber-reinforced polymer/Al7075-T6 stacks panel, tetrahedral amorphous carbon coated tools, single-shot drilling, process capability six pack analysis

Introduction

Superior qualities of composite materials, in comparison to known traditional equivalents, have generated a great deal of interest in utilizing them in a variety of applications, from the automobile to the aircraft sectors. The use of composite materials in the construction of aero planes has improved fuel efficiency, decreased emissions, and enhanced weight bearing capability.

Demand for multilayer metallic/composite stack up materials, i.e., applications made of carbon fiber-reinforced polymer (CFRP), titanium and/or aluminium has recently increased in the market. These materials are specifically used to carry heavy loads during the operation of aircraft.[1] Although the majority of composite constructions are often designed to adhere materials that are close to net shape, more complex components are also employed for assembly and require secondary machining operations. As of now,

drilling offers the most significant machining capability for incorporating screws and rivets into part assembly. However, drilling fiber-reinforced composite materials differs in several ways from drilling metallic materials and presents special obstacles because their manufacturing activity is different from metallic materials.[2–4] Therefore, obtaining

[1]School of Mechanical Engineering, Universiti Sains Malaysia, Nibong Tebal, Malaysia
[2]Department of Engineering Technology, Faculty of Technology, University of Jaffna, Kilinochchi, Sri Lanka
[3]Advanced Machining Lab, Melaka, Malaysia
[4]Laboratoire des Technologies Innovantes, Amiens, France

Corresponding author:
Muhammad Hafiz Hassan, School of Mechanical Engineering, Universiti Sains Malaysia, 14300 Nibong Tebal, Malaysia.
Email: mhafizhassan@usm.my

minimum defects in the hole is essential to enhance the life and functioning of an aircraft. Delamination and burr formation are two such hole edge defects which are to be minimized.

Delamination is regarded as the most serious damage of all the damages. It happens when the drill's thrust force is greater than the layers' interlaminar fracture toughness. In other words, it happens as a result of bending stresses between the drill bit and the material contact point leads to decreased structural integrity and poor assembly tolerance.[5] Drilling operations are known to induce delamination at both the entry and exit points of the workpiece.[6] The primary motivator for delamination during drilling were the thrust force and special drill geometry.[7,8] Krishnaraj et al. recognized two distinct forms of delamination: peel-up and push-down delamination.[3] As the drill moves forward, the upper layers of the material tend to lift-up during peel-up delamination mechanism rather than being sliced.[9] On the other hand, the indentation action, working across the uncut layers of the laminate, causes the push-down delamination. It was discovered that the delamination caused by push-down is worse than that caused by peel-up.[10] It is because, the high-temperature metallic chips reduce the bonding strength of the matrix, and cause damage to CFRP panel, which further exaggerates the delamination of CFRP.[11] However, placing a support plate under the work piece is the most well-known way to lessen this specific delamination.[12]

Another major problem that needs to be addressed is burr formation. The tool geometry, process parameters and drilling environment have big influence on burr formation during drilling. Burr formation results in a number of issues, including difficulty in attaching the parts, worker accidents during assembly, and the need for an additional deburring operation to remove the burrs. Due to the workpiece's plastic deformation, burrs develop on both the entry and exit sides of the hole. If the material is moderately ductile, burr development could happen because it has a tendency to elongate somewhat as a result of the heat created during drilling. The bottom surface layer of the alloy heated up as the drill bore through it, enhancing the Al7075-T6 alloy's ductility. The burr is then produced as the highly heated and ductile material flows in the direction of the exit hole.[13] The longer the tool takes to reach the work material, the higher the maximum burr height (H_{bmax}) value may be obtained since, H_{bmax} is positively dependent on the time interaction. Longer contact times during drilling will result in higher temperatures that will heat the cutting tool and degrade the quality of the hole.[8,14]

In contrast to other surface damage, the burr formation at the aluminium part's exit is a major issue for the CFRP/Al assembly since it frequently necessitates further stack disassembly, deburring, and reassembly. The deburring process would take up to 40% of the total machining time and account for approximately 30% of the overall assembly cost if burrs form at the exit drilled hole after the drilling process.[15,16] When the feed rate was raised during the drilling operation, Rivero et al., found the least burrs creation at the hole edge.[17] In contrast, Kim et al., and Gao et al., mentioned that exit burr height increases with the increase of speed.[18,19]

Carbon atoms can be arranged in three hybridized states such as graphite, diamond and tetrahedral amorphous carbon (ta-C). Graphite is characterized by 100% sp^2 and diamond is characterized by 100% sp^3 hybridization. Graphite has a hexagonal basal plane structure with strong covalent in-plane bonds and weak Van der Waals out-of-plane bonds, making its coefficient of friction (COF) low. In contrast, diamond is composed of a tetrahedral structure with each atom covalently connected to the other three atoms. This ensures an electrical insulator behaviour, an extremely effective thermal conductivity and the highest level of hardness attainable in nature. The ta-C structure is a hybrid of sp^2 and sp^3 whose ratio determines its properties.[20] The film structure was described as somewhat crystalline with diamond-like lattice characteristics. Aisenberg and Chabot stated that, using ta-C coatings improved the cutting ability of paper-cutting blades.[21] When the blades were examined for wear, the frictional coefficient was reduced. Also, it was noted that a 2 μm ta-C coating increases stainless steel's resistance to abrasive wear, extending the material's lifespan from a week to 85 years.[22]

Ta-C has a number of advantageous features that make it suited for stack up drilling. It has a lower coefficient of friction, providing superior resistance to adhesive wear and tribo-oxidation. This property also enhances its high-stress resistance under deficient lubrication and dry running conditions. The extreme coating hardness of ta-C provides outstanding protection against abrasive wear. In addition, the inert surface chemistry of ta-C ensures smooth-running behaviour, reduces sticking, eliminates demoulding problems caused by deposits and exhibits improved corrosion resistance. All these improved qualities lead to wear reduction on heavily stressed surfaces, extended service life of the components and boosts the productivity of the manufacturing process.

Research on the effect of alloying ta-C with transition metals like Ti[23,24] and Cr[20] was already been tried by researchers. Ta-C is a brittle ceramic, and alloying with stable carbide-forming metals causes the growth of nanoscale carbide inclusions, which make the material harder [22]. Alloying with transition elements (particularly group IIB, IIIB and IVB) is usually occupied to enhance the mechanical strength of the films by enhancing the adhesive strength between ta-C and substrate.[25] By reducing the stress on the film, intermediate layers may adhere well.[26]

Franz et al., provided a review of the most recent investigations on the effect of coatings on the overall

performance when drilling CFRP/Al stacks.[27] It can be noticed that the impact of the selection of tool coating on the overall drilling performance for such multi-material stacks, widely used in aerospace applications and particularly in commercial aircraft, has received insufficient research attention. Hence it is essential to conduct research on how well these stacks perform during drilling operations using coated tools. The application of nanocomposite ta-C coating with binders, which is more cost-effective than other coatings for drilling stack materials in a single-shot drilling method, has not yet been attempted. To achieve superior drilled-hole quality, it is crucial to investigate the basic understanding of the study parameters and the interactions between the parameters, including the bonding force mechanism and hole quality features. Therefore, this research focuses on finding a suitable coating to improve the hole quality in terms of delamination and burr formation.
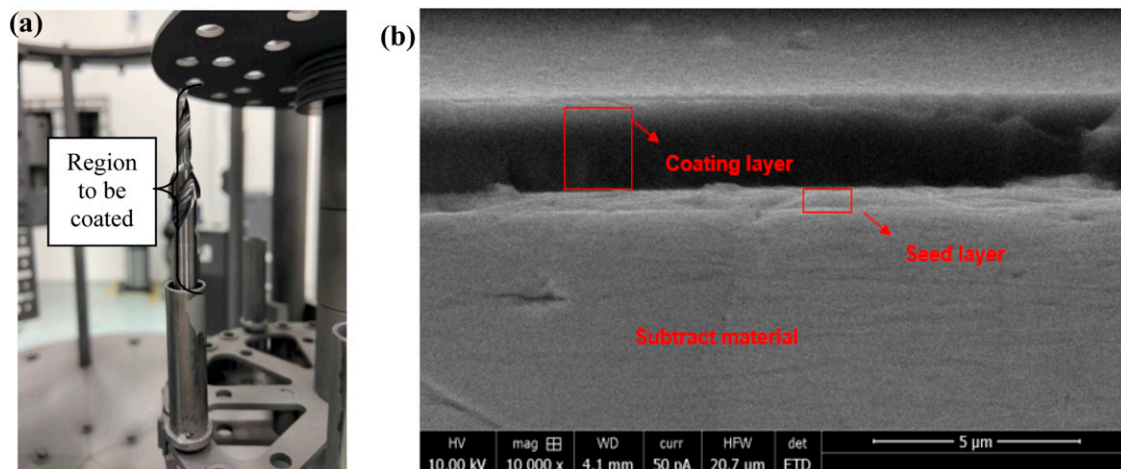
Methodology

Materials

In this research work, experiments were performed on a multi-material stack composed of 3.25 mm thick CFRP, manufactured by Composite Technology Research Malaysia (CTRM) with a stacking sequence of $[45/135/90_2/0/90/0/90/0/135/45_2/135]_s$ and nominal fiber volume fraction of 60%, and 3.317 mm thick 7075-T6 aluminum alloy (Al7075-T6), which contains approximately 92.459 wt% aluminum, 2.696 wt% magnesium, and 4.845 wt% zinc. A 0.08 mm thin layer of glass/epoxy woven fabrics was used at the top and bottom of the CFRP laminate to prevent delamination at both the entrance and exit of the hole during drilling. The final thickness of the whole composite panel, including the paint application, was 3.587 mm.

The CFRP was compacted using a vacuum pump under controlled atmospheric conditions during the curing process. The entire cure cycle was carried out in an autoclave at a pressure of 700 kPa and placed in a vacuum bagging that was depressurized to 70 kPa. It involved raising the temperature by 3°C/min to 180°C, where it dwelled for 120 min, then reducing the temperature at the same rate until it reached room temperature. The dimensions of the stack were 185 mm x 85 mm. The properties of CFRP used here are as follows; tensile strength is 2723 MPa, elasticity module is 164 GPa, elongation percentage is 1.62, flexural strength is 1500 MPa, interlaminar shear strength is 80 MPa, density is 1.601 g/cm^3 and hardness is 180 HV.[28,29]

Cutting tool

Due to its excellent wear resistance while drilling abrasive materials like CFRP, a sintered rod of tungsten carbide (WC) was chosen as the drill bit material. Furthermore, WC has the advantage of having a Vickers hardness value (1625 HV) and density (14.35 g/cm^3) much higher than those of the workpiece. The tungsten carbide rod was made up of 93.36 wt% WC and 6.64 wt% Cobalt (Co). A tool with a diameter of 4.85 mm, 45° of chisel edge angle, 6° of primary clearance angle and 130° of point angle was used in this study.[29] The drill bits are manufactured by Gandtrack Asia Sdn. Bhd. The twist drill was designed using Helitronic Tool Studio version 1.9.216.0 software (Walter Maschinenbau GmbH, Garbsen, Germany).

The drill bits were coated using the physical vapor deposition (PVD) method at Surtreat Solutions Sdn. Bhd, Johor, Malaysia. Triple rotation in the PVD coating machine is occupied to perform the task, Figure 1(a). The total thickness of the ta-C composite layer measures approximately 2 μm, with an additional dopant layer that is 0.5 μm thick as shown in Figure 1(b). Four types of drill bits were

Figure 1. (a) Drill bit set up for PVD coating process (b) SEM observation of the formation of a ta-C and seed layer this is subsection of methodology section after cutting tool section

produced: uncoated, micro-tetrahedral amorphous carbon coated (ta-C), chromium dopant added tetrahedral amorphous carbon coated (ta-C:Cr), and titanium dopant added tetrahedral amorphous carbon coated (ta-C:Ti), to experiment with the effect of dopant layer on the coating performance of tetrahedral amorphous carbon layer.

Drilling process

Drilling tests were carried out in a dry single-shot process, starting from the CFRP to the Al7075-T6 panel, by using a computer numerical control (CNC) machine (Fanuc Robodrill T21iFLb), which has a variable spindle speed up to 10,000 rev/min and spindle drive motor power of 3.7 kW. For a regular rate, the feed rate can range from 1 to 30 mm/min, and for a high transverse rate, it can range up to 48 m/min (x, y, and z axes). As illustrated in Figure 2, the stack panels were slotted into the jig fixture (144.37 mm x 78.06 mm x 20 mm) and clamped there. Figure 3(a) shows the separated workpiece after drilling all 100 holes and Figure 3(b) shows the cross section of a drilled hole.

In this work, the effect of dopant layer on the coating performances of different ta-C coated tools was investigated using a spindle speed of 2600 rev/min and a feed of 0.05 mm/rev for all runs since these parameters gave best outputs in the earlier experiments.[28] Dry drilling conditions are employed to imitate the drilling process that actually occurs during panel manufacturing. Although the use of cutting fluids can increase machining effectiveness and extend tool life by dissipating heat generated at the cutting region, the repeated use of coolant in composite-metal stack drilling processes is uneconomical and unfriendly to the
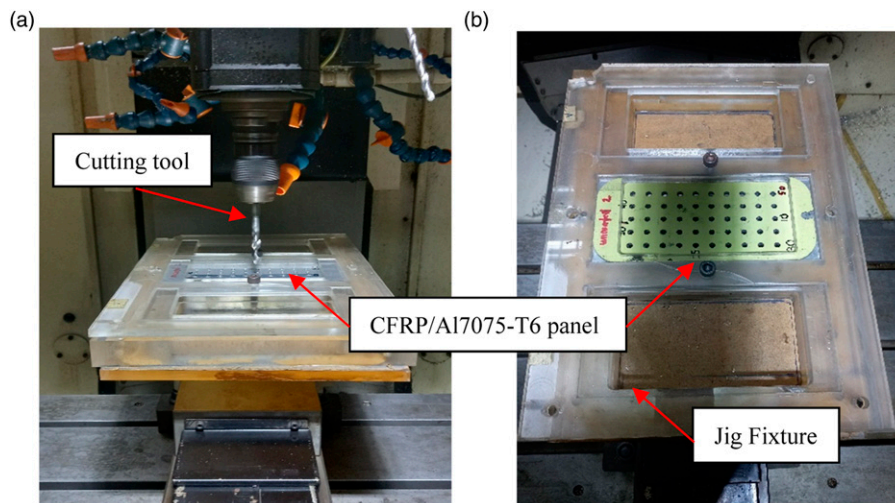
Figure 2. (a) Set-up for single-shot drilling process (b) drilling sequence from the 1st until 50th hole.
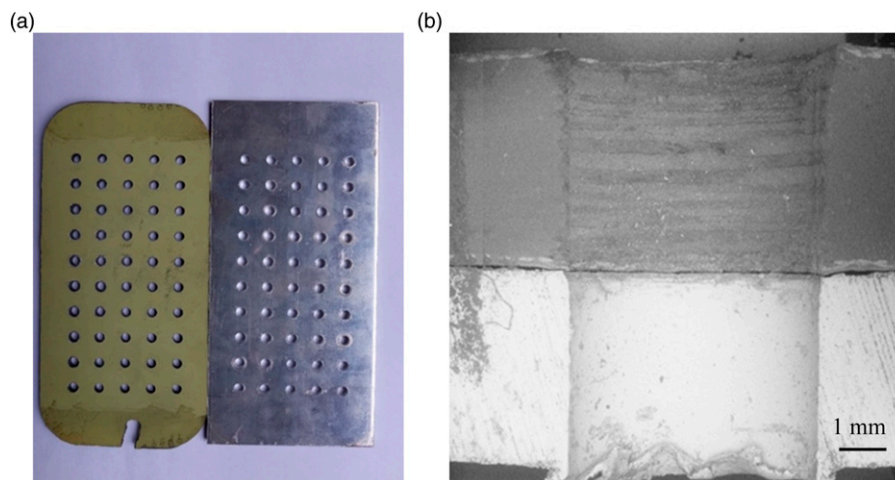
Figure 3. Illustration of (a) drilled workpiece (b) Cross section view of stack panel.

environment due to the heavy pollution of the powdery carbon fiber reinforced polymer's chips, which justifies the desire to reduce its use.[28] Additionally, it is interesting to reduce the amount of cutting fluid used to prevent the need for post-drilling cleanup.

Coating characterization

Both nano scratch and indentation tests were used to characterize the nanocomposite coating. These tests were conducted using a Nano Test Vantage machine (Micro Materials Ltd), as shown in Figure 4. The micro hardness test was then defined, and all the parameters were set and the machine was allowed to run.

Nano scratch test was performed in multi-pass wear experiment mode (3 passes repeated for 4-5 times), with the parameters set given in Table 1. The set of parameters used for nano indentation test are summarized in Table 2.

The experimentation sample should have fine surface finish and should be free from any dirt or grease as these irregularities may affect the readings. Graph of friction force versus distance was obtained, and the values of coefficient of friction and hardness were also obtained for further analysis.

Drilled-hole quality

CFRP delamination. In the context of CFRP laminate production, delamination, particularly at the exit side of drilled holes, is regarded as a critical quality concern. This defect at the hole's edge can be effectively addressed at the entry side through secondary processes like countersinking or counterboring.[30] In this study, delamination was assessed at the exit side of the CFRP panel after the single-shot drilling process by using an Alicona Infinite Focus optical microscope (IFM) at 5x magnification, as depicted in Figure 5(a). A close-up view of delamination is given in Figure 5(b).

To assess the extent of drilling-induced delamination, researchers have introduced the widely recognized delamination factor, denoted as F_d.[31–36] F_d is defined as the ratio of the maximum diameter D_{max} of the observed delamination zone to the nominal diameter of the drilled hole D_{nom}. To ensure that delamination amount is within the accepted industrial limits, the difference between the nominal diameter D_{nom} and the maximum damage diameter D_{max} observed at the exit side of the CFRP part must be less than 1 mm, as preconized by the leading tool manufacturer Sandvick Coromant,[37] which corresponds to a value of F_d equals to 1.206 for a nominal diameter D_{nom} of 4.85 mm chosen for this study.

Burr formation. To reduce difficulties during fastener positioning and riveting, and lower manufacturing costs, it is necessary to reduce the size of burrs observed more significantly at the periphery of the drilled hole at the exit side of the aluminium panel (Figure 6(a) and (b)). The maximum height H_{bmax} of the burr formation can be identified from the 3D image produced by the Alicona IFM, with a 5x magnification, by marking the highest burr point with a red line, as shown in Figure 6(c).

According to Dornfeld et al., Kurfess et al., and Franke et al., the burr formation limit at the interface of drilling stack-up materials should not exceed 150 μm, otherwise an additional operation called deburring must be carried out when installing rivets or other fasteners.[38–40]

Process capability six pack analysis

It is important to differentiate between a process's ability to produce parts that meet engineering standards and its ability to consistently maintain the control over the range of products. To compare different processes, a commonly used formula is employed in this study to determine the capability of the process which is process capability six pack analysis. Process capability is a measure of process performance that is an indication of the ability of the process to reliably manufacture a product or component.[39] Process
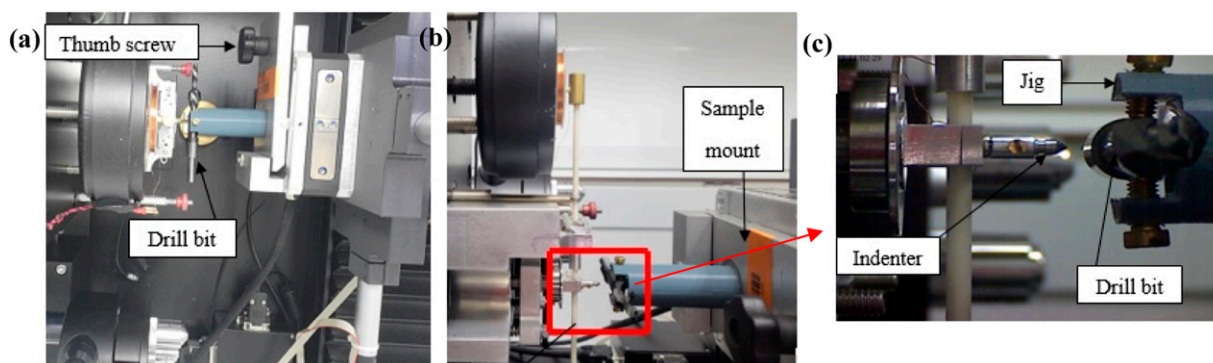

Figure 4. Set-up for nano indentation and scratch tests: (a) top view, (b) side view, (c) close-up view.

capability six pack analysis, consisting of individual control chart (I chart), moving range chart, capability histogram, normal probability plot and capability plot, is occupied in this study to statistically analyze the process control from the data (factor delamination F_d and maximum burr height H_{bmax}) obtained by the experiments. By highlighting out-of-control data points, patterns, and trends, control charts assist in monitoring the stability of the process. Red dots in individual control chart (I chart) represent the points which are not under control and failed. Out-of-control points imply that the operation may not be consistent and that the results of a capability analysis may not be reliable. The upper and lower control limits of the I chart, respectively denoted UCL and LCL, are given by equations (1) and (2):

$$UCL = x + 3\sigma \qquad (1)$$

Table 1. Nano scratch test parameters used in this study.

Parameter	Value
Limit stop load [mN]	0.2
Scratch load [mN]	250–500
Loading rate [mN/s]	15
Scan length [µm]	300
Scan velocity [µm/s]	9.2
Space in Y-direction [µm]	80
Retraction distance [µm]	25

Table 2. Nano indentation test parameters used in this study.

Parameter	Value
Maximum load [mN]	50
Loading/unloading rate [mN/s]	5
Dwell time at maximum load [s]	6
Gap between each indentation point [µm]	15

$$LCL = x - 3\sigma \qquad (2)$$

where $\overline{x}$ is the arithmetic mean of the total data, σ represents the standard deviation of the data within the specification.

In moving range chart, moving range (MR) values of 11 observations were reported and represented as a function of the observation number according to equation (3). The first observation is performed on the 1st hole and the following observations are made with an interval of 10 holes, from the 10th hole to the 100th hole. MR is calculated as the difference between the value of consecutive controlled data (factor delamination F_d and maximum burr height H_{bmax}):

$$MR = x_{i+1} - x_i \qquad (3)$$

Where x_i is the data of the ith observation ($i = 1,2;3; 4…;10$).

In the capability diagram, upper and lower specification limits, respectively denoted USL and LSL, are given by the customer. LSL represents the lower value of the studied process parameters. Thus, a drilled-hole without delamination at the exit side of the CFRP panel is characterized by a value of one for F_d. If there is no burr formation at the periphery of the drilled hole at the exit side of the aluminium panel, H_{bmax} equals 0. USL represents the acceptable limit of the studied process parameters. As explained in section 2.5, a maximum value of 1.206, respectively 150 µm, is preconized for F_d, respectively H_{bmax}.

Ideally, all of the data fall inside the permissible ranges and the data spread is less than the specification spread. Data that fall outside of the specification's bounds are considered nonconforming. Parts per million (PPM) can be used to calculate the precise number of nonconforming pieces in the process. If the normal distribution is an excellent match for the data, the points form an almost perfectly straight line and fall along the best - fit line, which is located between the confidence bounds in the normal probability plot. This straight line is a good indicator of deviations from normality. A normal distribution of the data can be assumed if
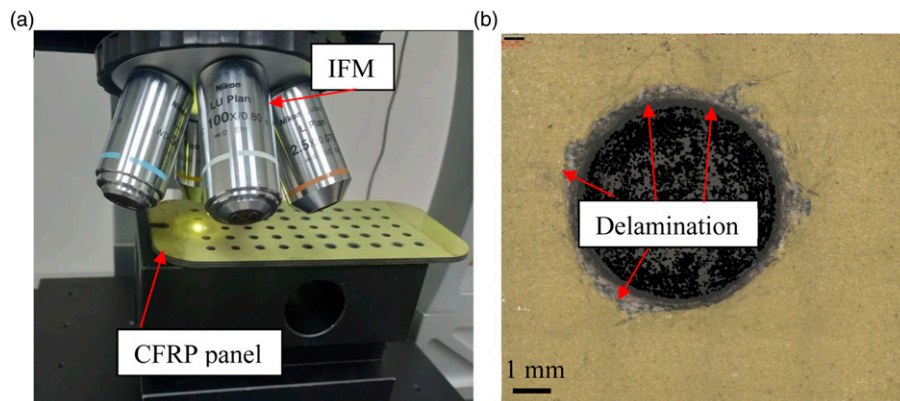
Figure 5. (a) Alicona IFM, (b) close-up view of drilling-induced delamination at the exit side of the CFRP panel.
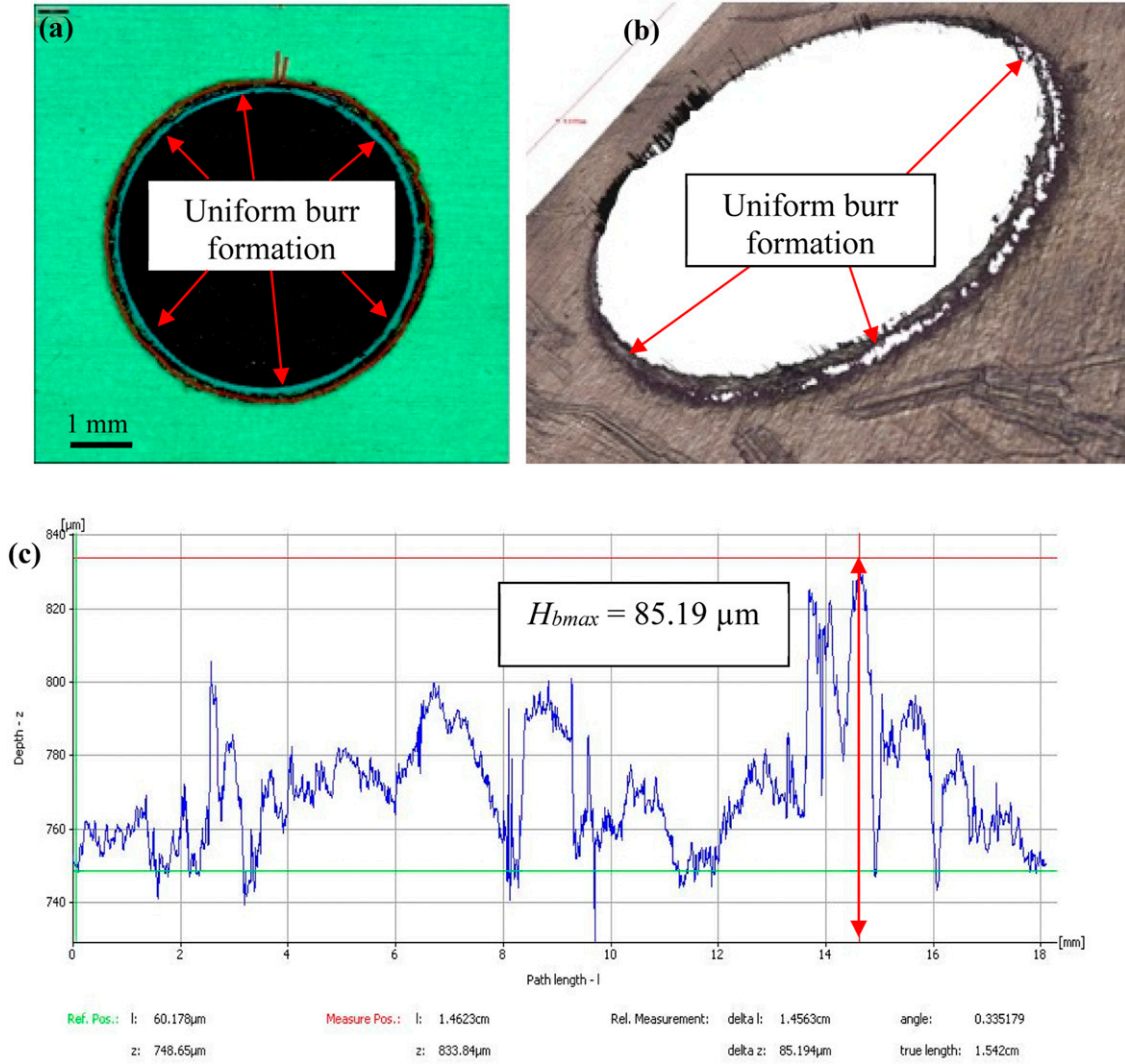
Figure 6. Measurement process of maximum burr formation: (a) 2D observation of entrance burr formation (b) maximum burr formation identification by Alicona IFM, (c) maximum burr formation measurement.

the *p*-value is greater than 0.05. The results of the capability analysis may not be reliable if the *p*-value is less than 0.05 because it indicates that the data are not normal. The degree to which the data adhere to a specific distribution is determined by the Anderson-Darling (AD) statistic. In general, the smaller the AD statistic is, the better the distribution fits the data.

The capability ratio C_r can be considered as a gauge of how much of the designer-specified tolerance range is impacted by manufacturing process variation. In other words, this is how the tolerance between what one can make and what one will accept for the goods compares. C_r is calculated as follows [39]:

$$C_r = \frac{6\sigma}{USL - LSL} \quad (4)$$

The process capability C_p is the reverse of C_r. A C_p value of 1.33 or higher is typically regarded as sufficient. The process measurement also needs to consider whether or not the distribution is centred around the mean. That is, even if the production is biased to the point that it is completely outside of the range of the specification, computing a ratio can still yield a decent value for the indices.

C_{pk} is a more suitable measurement to employ because it reveals whether the process is able to adhere to limits and whether it is centred around the desired target value. C_{pk} can be calculated as follows:

$$C_{pk} = \frac{Z_{min}}{3} \quad (5)$$

Where z_{min} corresponds to the minimum of the difference between Z_{USL} and Z_{LSL}. The relationship between the upper,

respectively lower, specification limit in units of standard deviations and the process means, $\bar{x}$, is given by equation (6), respectively equation (7):

$$Z_{USL} = \frac{USL - \bar{x}}{\sigma} \qquad (6)$$

$$Z_{LSL} = \frac{\bar{x} - LSL}{\sigma} \qquad (7)$$

The process will be considered valid if the value of C_{pk} is greater than 1.00. When the process is out of tolerance, C_{pk} will be negative, which means that more than half of the production will not meet requirements. Based on the process location and dispersion, the P_{pk} value is used to assess the process overall capabilities. The process overall capacity shows how it has actually performed throughout. Higher P_{pk} levels often denote a more capable operation. Lower P_{pk} readings suggest that the operation could be improved. If P_p and P_{pk} are approximately equal, the process is centred between the specification limits.

Results and discussion

The results of the characterization of coatings in terms of hardness, scratch resistance and coefficient of friction are discussed in this section. Along with it, the study on drilled-holes quality is presented and discussed with supporting evidence. These results are further supported by process capability six pack analysis report wherever necessary.
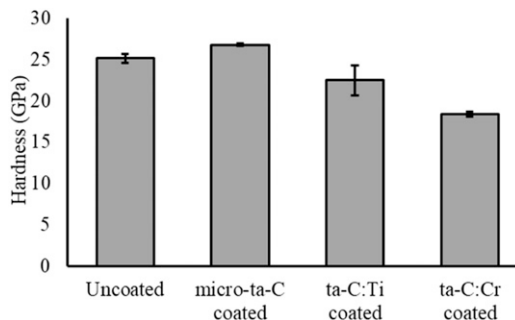

Figure 7. Microhardness values for all tools.

Coating characterization

Microhardness. Since the properties of thin films are generally different from that of the bulk materials, it is advisable to measure the properties of deposited thin films of ta-C during experiments.[41] Similar to research Oliver et al., nano test machine was used in this study to measure the microhardness of coatings.[42] As shown in Figure 7, the $HV_{0.005}$ hardness values of drill bits with three different ta-C coating-types were compared to that of uncoated tool. It was found that the deposition of micro-ta-C coating layer increased the hardness of cutting tool (26.78 GPa) compared to that observed on uncoated drill bit (25.15 GPa). Similar range of 20–29.1 GPa were found in the literature for ta-C coating at varying loads of 10–70 mN.[25,43,44] Moreover, it can be noted the addition of metallic dopants, i.e., chromium or titanium, deteriorated the hardness of cutting tool. We measured a hardness value of 22.5 GPa for ta-C:Ti coated tool, in agreement with the results found at lower critical load (10 mN) in the scientific literature.[23,45] According to this study, the ta-C:Cr coated tool exhibited a hardness value of 18.41 GPa. This figure surpasses the measurement reported by Fiaschi et al., which ranged from 2.5 to 3.5 GPa at a 100 mN load. This difference can be explained by the low amount of sp^3 hybridized atoms (around 50%).[20]

Scratch resistance. Scratch tests were performed in order to determine the maximum bonding strength of coating with tool. If the coating is deteriorated too quickly, the expected performances in terms of wear resistance will not be reached, which in turn affects the hole quality. Figure 8 displays the scratch diagrams acquired under microscope for each of the three types of drill bits after the scratch test. Significative damaged areas can be observed after scratch tests performed on micro-ta-C and ta-C:Cr coated tools (Figure 8(a) and (b)), while few deterioration of the surface was detected for ta-C:Ti coated drill bit (Figure 8(c)).

To evaluate the ability of the coating layer to remain stuck on the cutting tool, and thus ensure that it correctly plays its role of delaying the apparition of the tool wear, maximum bonding strength of the selected coatings were assessed and the effect of the ta-C coating type on the
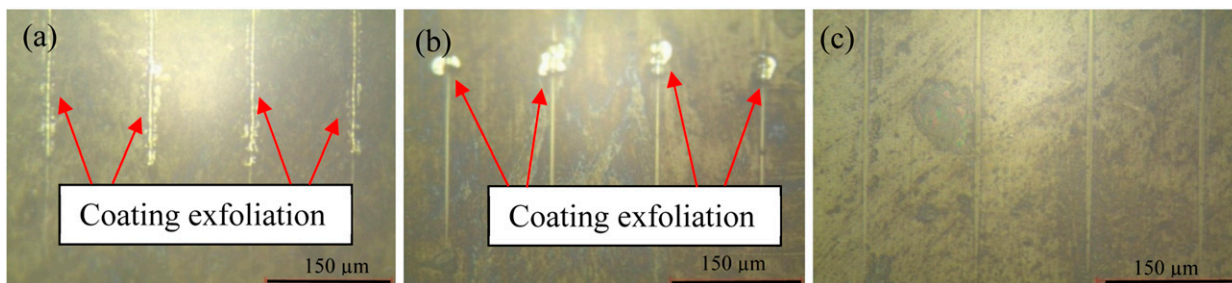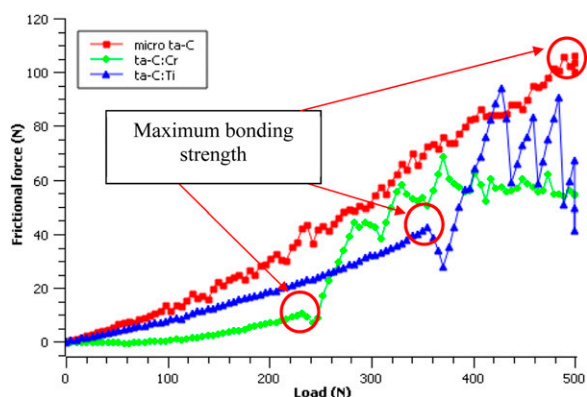

Figure 8. Variation of scratch with distance under 250 mN for (a) micro-ta-C coated, (b) ta-C:Cr coated and (c) ta-C:Ti coated drill bits.

evolution of the frictional force was plotted as a function of the applied load in Figure 9. It was found that a correlation exists between the bonding strength of the coating and its ability to resist separation from the substrate under the application of frictional forces. Coatings with higher bonding strengths are less likely to exfoliate from the substrate under frictional stress, which results in lower coefficients of friction. The maximum points marked by circles in the graph are the points where the maximum bonding strength was obtained. The signals obtained after this point are the signals generated while scratch is made on the bare tool where coating is already failed and it is the reason for the scattering of the signal.

Table 3 provides the maximum frictional force and bonding strength values obtained for each ta-C coatings tested in this study. It was found that the coating layer with chromium dopant (ta-C:Cr) exhibited the weakest adherence, with a maximum bonding strength of 231.93 mN, while the adhesive strength of ta-C:Ti and micro-ta-C was roughly 1.5 and 2 times stronger, respectively, compared to ta-C:Cr. The maximum bonding strength of 355.49 mN evaluated for the coating layer with titanium dopant (ta-C: Ti) is in agreement with the adhesive strength values found by Zhang et al., which ranged from 359 to 381 mN.[45]

Coefficient of friction. Coefficient of friction (COF) is calculated by dividing the frictional force by applied load from the values obtained using Nano Test Vantage machine. It is studied in this research since it affects the burr formation. When the coefficient of friction between drill bit and workpiece becomes higher, the temperature rises, which in turn increases the ductility of the aluminium panel and finally results in higher burr height formation. Figure 10 shows the comparison of coefficient of friction (COF) values of all the drill bits. Ta-C:Cr coating produced minimum coefficient of friction curve (less than 0.05) and it is followed by ta-C:Ti coating (0.05 – 0.09). Though uncoated (0.06 – 0.15) and micro-ta-C (0.1 – 0.2) coated drill bits produced higher coefficient of friction, their values are less than 0.2 which shows a good compatibility of the tool for the expected job.

Drilled-hole quality analysis

CFRP exit delamination. As mentioned by Feito et al and Zhong et al., the thrust force contributing throughout the drilling process causes the exit delamination to be greater than the entry delamination.[4,46] Thus, current study focused only on delamination at the exit side of the CFRP panel.

Figure 11 gives the exit delamination factor value obtained after various numbers of drilled-holes with uncoated or coated cutting tools. Thus, it is possible to compare the drilling performance of each ta-C coatings tested in this study. It can be noted that the uncoated tool was not fit for single-shot drilling of CFRP/Al7075-T6 stacks with the cutting conditions used in this study, since almost all the drilled-holes exhibited delamination level superior to the accepted industrial limits, corresponding to delamination factor of 1.206. At the contrary, micro-ta-C coated tool proved its ability to drill until 90 holes with exit delamination below the expected industrial tolerance. It can be explained by the reduction of wear probability due to the high hardness and high bonding strength of this coating type. High hardness can spread out and reduce thrust force, and a reduced thrust force can efficiently result in a lower

Figure 9. Effect of the ta-C coating type on the evolution of the frictional force as a function of the applied load.

Table 3. Maximum frictional force and bonding strength for the coatings of this study.
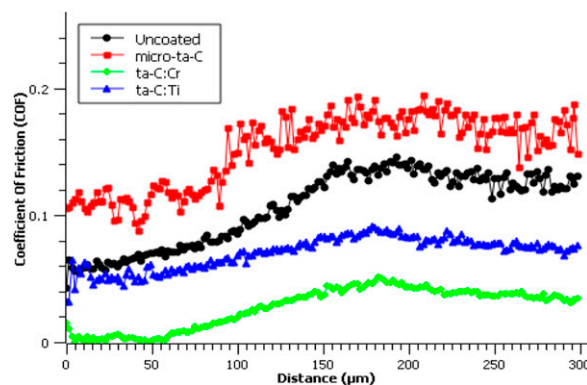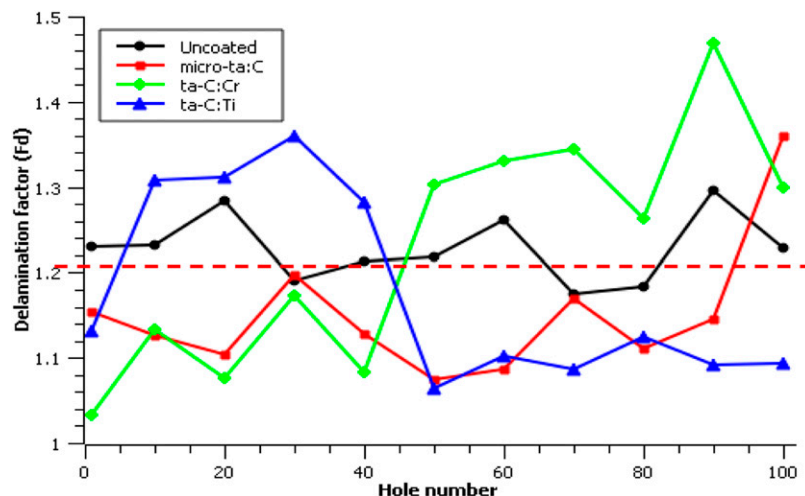
Coating	Maximum frictional force [mN]	Maximum bonding strength [mN]
Micro-ta-C	110.44	500
Ta-C:Cr	10.52	231.93
Ta-C:Ti	42.66	355.49

Figure 10. Effect of the ta-C coating type on the evolution of the coefficient of friction.

Figure 11. Evolution of delamination factor at the exit side as a function of the number of holes drilled by uncoated and coated tools.

delamination factor to improve the drilled hole's quality. Due to high bonding strength, tool wear slows down and in turn the delamination is limited. Similar results were found by Zhong et al., since the amount of delamination obtained with uncoated tool in their work was almost 4 – eight folds that of TiAlN coated tool.[46] The ta-C coating is not completely exfoliated even after 100 holes and the presence of coating on the tool surface of the micro-ta-C coated drill is confirmed by energy-dispersive X-ray (EDX) analysis, as shown in Figure 12. Moreover, the choice of the metallic dopant (i.e. Cr or Ti) induced dissimilar behaviour in terms of exit delamination evolution as a function of the number of drilled-holes. Ta-C:Ti coated tool produced drilled-holes with acceptable quality after 40 holes while ta-C:Cr coated tool produced 40 holes with delamination factor below 1.206 before crossing the accepted quality limit. The increase of delamination factor with hole number for ta-C:Cr coated tool is attributed to two reasons. First, the degradation of ta-C:Cr coated tool quality, due to the peel-off of the coating, is faster compared to the other tested tool coatings since the bond strength of this type of coating is minimum among all the tool coatings (Table 3). Second, the hardness of ta-C:Cr coating is minimum among all the tools and therefore it failed to spread out and reduce the thrust force, and hence resulted in higher delamination factor (Figure 7).

When comparing the delamination factor F_d which is shown in Figure 11 throughout the experiment, uncoated and micro-ta-C coated tools produced almost unchanged dimensions pattern. Ta-C:Ti coated tools shows a decreasing delamination trend of 16.35% while ta-C:Cr shows an increasing trend of 20.47% comparing the start and the end of the process. These results are better compared to the experiment conducted by D'Orazio et al., as they obtained the F_d value of first hole to be 55.5% and 50% lower than the

value of last hole for the DLC coated, and TiAlN coated drills respectively.[47]

Delamination factor F_d obtained at the CFRP exit side from the experiments are then analyzed by process capability six pack analysis to statistically investigate the process control. Individual control chart (I chart), moving range chart, capability histogram, values of all observations, normal probability plot and capability plot are summarized in Figure 13 for uncoated and micro-ta-C, ta-C:Cr and ta-C:Ti coated drill bits.

First, the analysis of the results presented in I-charts shows that the drilling process is under control for the uncoated and coated tools of this study since all the points are between the control limits (except for the 100th drilled hole produced by micro-ta-C coated tool (observation 11 in Figure 13(b)) and the 30th drilled hole produced by ta-C:Ti coated tool (observation four in Figure 13(d))). The mean values of F_d obtained with micro-ta-C an ta-C:Ti coated tools on the overall of the hundred drilled-holes are under the accepted limit (i.e. $\bar{x}$ = 1.1506 and 1.1775 in Figure 13(b) and (d) respectively) while this value is over 1.206 for uncoated and ta-C:Cr drill bits (i.e. $\bar{x}$ = 1.2282 and 1.2276 in Figure 13(a) and 13(c) respectively). Moreover, it can be noted that, more than half of the holes drilled by uncoated and ta-C:Cr coated tools exhibit delamination at the CFRP exit side outside the specified range as shown in the capability histograms (Figure 13(a) and 13(c) respectively). This conclusion is confirmed by the negative value of P_{pk} and C_{pk} obtained for these two tools, which means that the process is out of tolerance in these both cases. Thus, we can already conclude that uncoated and ta-C:Cr coated drill bits are not qualified to meet industrial requirements in terms of extent of drilling-induced delamination generated at the exit side of the CFRP panel after the single-shot drilling process of CRFP/Al7075-T6 stacks.
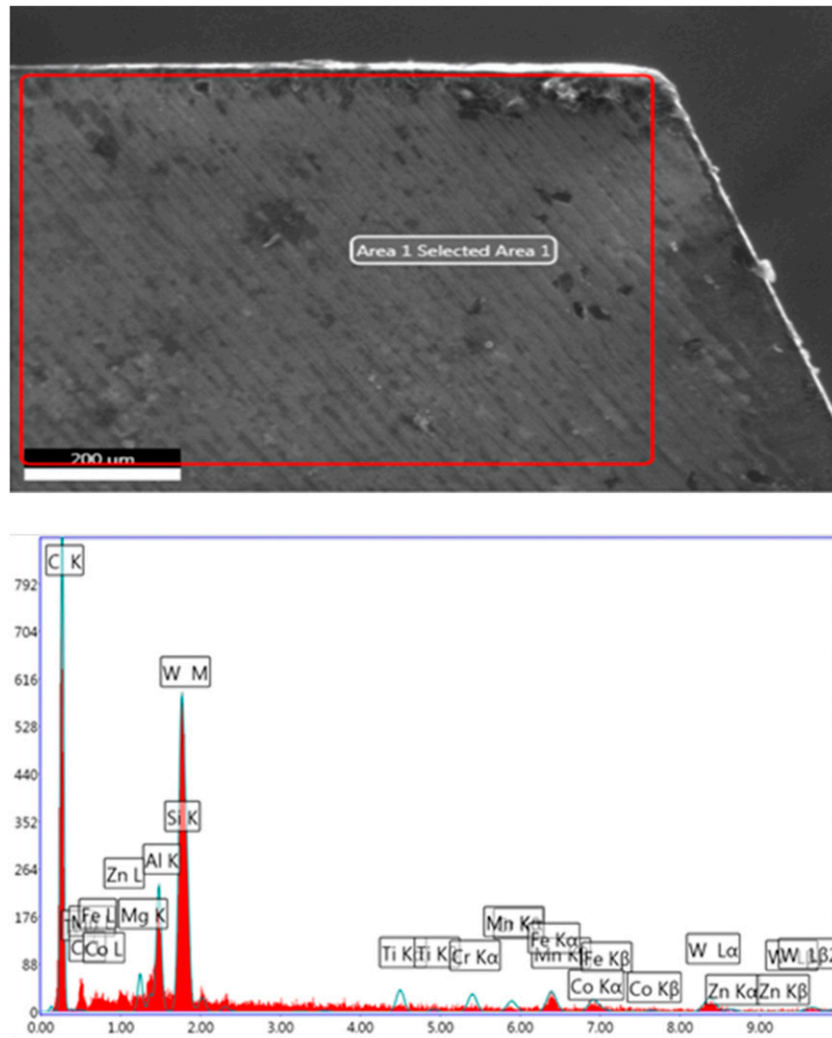
Figure 12. ESEM/EDX analysis of the micro-ta-C coated tool at the 100th drilled hole.

Though the exit delamination observed at the holes drilled using micro-ta-C coated tool follows the normal distribution curve according to histogram (Figure 13(b)), it doesn't fit well within the specified limits, because one value fall well outside the confidence interval in normal probability plot and in the histogram. It can also be stated that, since the *p*-value is less than 0.05 and the Anderson-Darling (AD) statistic value is quite bigger (0.875), the data does not follow the normal distribution well. However, the results of the capability plot obtained with micro-ta-C coated tool (Figure 13(b)) are better than those of ta-C:Ti coated tool (Figure 13(d)). Thus, it can be considered that micro-ta-C coated drill bit turns out to be the best choice among the cutting tools tested in this study when considering the minimal extent of drilling-induced delamination generated at the exit side of the CFRP panel after the single-shot drilling process. However, the process capability six

pack report also shows that the process can further be improved.

Burr height formation. Though burr may be created at the entrance and exit of the Al7075-T6 panel, current study was focused only on the exit side burr formation since the entry side is not significant due to the compaction force from CFRP panel as stated by Sridar et al.[48] The 3D image was seen under the Alicona Infinite Focus Microscope under 5x magnification, and it shows that the burr formations were all uniformly distributed throughout the holes' perimeter. As a result of the cumulative heat from the CFRP panel, which enables the softened Al7075-T6 to be extruded at the tool margin area, burrs are anticipated to form. The compression rates in the hole's centre are often cause to the burr formation near the exit. Based on the fracture mechanism, the type of burr generation was classified during drilling
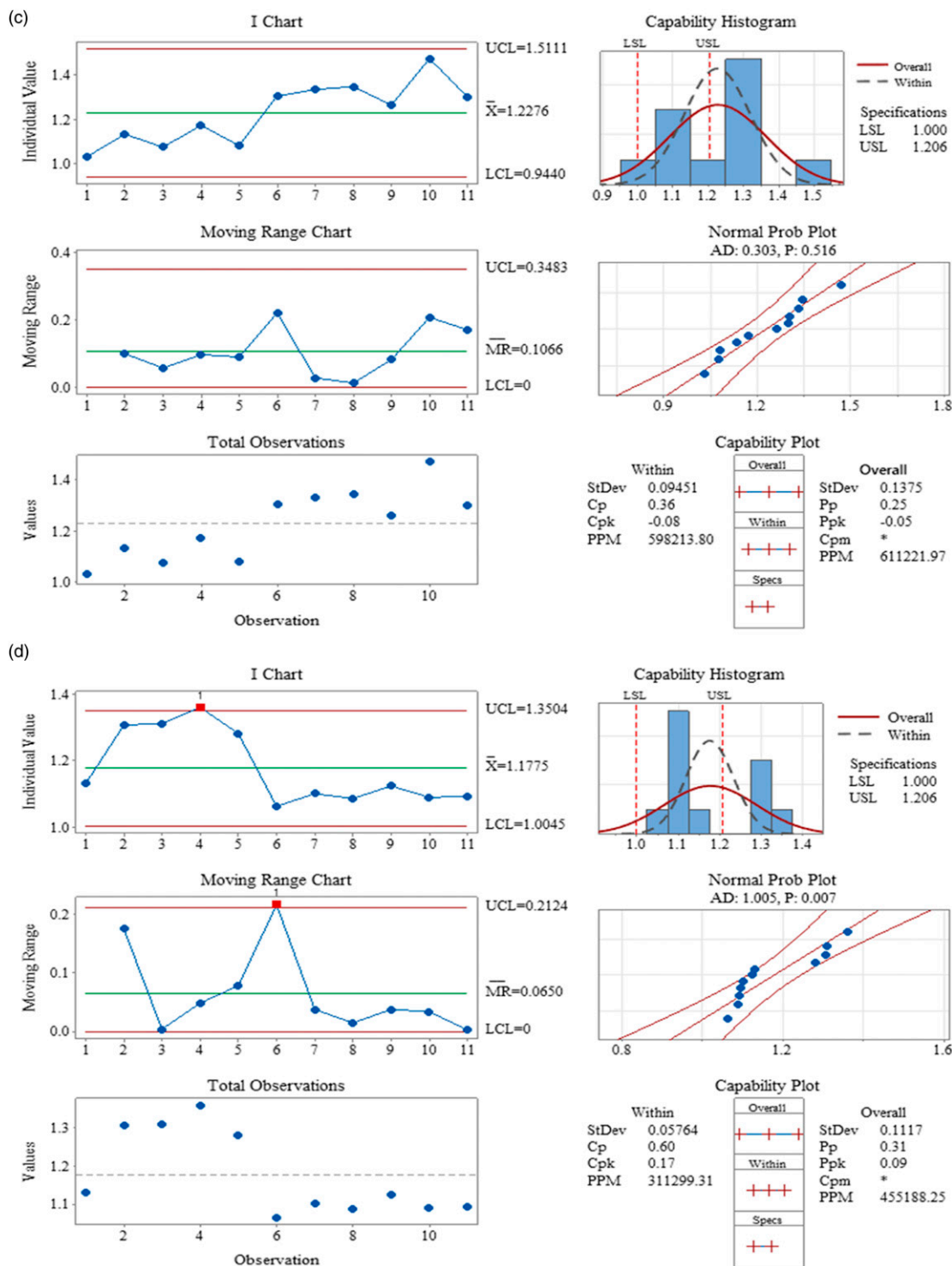
Figure 13. Process capability six pack report for the delamination of the holes drilled by (a) uncoated, (b) micro-ta-C coated, (c) ta-C:Cr coated, and (d) ta-C:Ti coated tools in CFRP.

Figure 13. Continued.

process. To produce a drill cap and uniform burr formation, the primary and secondary fracture must occur at distinct stages.[49] The residual material is twisted and pushed out in front of the drill to create a consistent burr with a drill cap after the initial fracture occurs at the end of the cutting edges.

The elevated range of burr height is because of the material property of the Al7075-T6 panel in the workpiece,

that the burr height would be higher the more ductile the material was.[50] The key mechanical attribute that defines the shape of the burr is the material's ductility, hardness, and tensile yield strength.[51] In their work, Bahçe and Özdemir obtained uniform burr on Al7075 holes during drilling operations and they claimed that it was probably caused by the material's high ductility, strength, and deformability.[52] It has also been noted that, using drills with large tip angles (such as 120° to 140°) results in greater localized plastic deformation along the hole's perimeter, which starts the production of cracks and burrs.[53,54] However, Dahnel et al. demonstrated that cooling reduced burr height by 10%.[55] These previous data show that the higher the ductility, the higher the burr height.

As can be seen in Figure 14, the overall observation of the burr height for all the tools ranges from 18.733 µm to 203.42 µm. Most of the holes produced by all the tools have exit burr height less than acceptable burr height of 150 µm. A criterion of maximum burr height H_{bmax} of 150 µm was used as the acceptance limit in this research work, in agreement with the value commonly found in the scientific literature to track the effectiveness of the cutting tool coating.[38–40] ta-C:Cr coated tool produced better burr height which is less than 150 µm throughout the operation among all the tools. Coefficient of friction (COF) is the reason in the current study to the less burr height formation of ta-C:Cr coated tool since it produced the lowest COF. Less COF leads to less rubbing of tool with the workpiece surface and therefore less temperature generation and in turn low ductility at the hole edge. Micro-ta-C coated tool has the maximum coefficient of friction and it produced the maximum average burr height of 126.75 µm. Uncoated, ta-C:Cr coated and ta-C:Ti coated tools produced

an average exit burr height of 103.11 µm, 96.4 µm and 118.56 µm respectively.

The burr height in the current experiment is improved compared to the results obtained by Hassan et al., while they're using the same drilling conditions.[56] Indeed, they mentioned that the burr height ranged from 133.62 to 211.45 µm when drilling CFRP/Al7075-T6 stacks using uncoated tungsten carbide drill with point angle of 130°. According to Hassan and Razali, TiAlN coated drill bits outperformed uncoated drill bits by maintaining the burr height below 80 µm.[57] They added that, it was evident that the burr height formed by both drills expanded steadily from the first hole to the 60th hole However, after the 70th hole, the uncoated drill's burr height measurement climbed significantly from 128 µm to 327 µm but the maximum burr height for the TiAlN tool was consistently held below 100 µm until the 81st hole.. It is certainly due to the coating that prevented the aluminium chip from forming BUL and BUE after being permanently placed at the tool surface. Similar tendencies could be found when drilling Ti/CFRP/Al stacks since Kuo et al., showed that the entrance and exit burr height produced by TiAlN/TiN coated drill bit reached up only to 150 µm whereas it came to 200 µm with the uncoated one.[58]

Maximum burr height H_{bmax} generated at the periphery of the drilled hole at the exit side of the aluminium panel from the experiments are then analyzed by process capability six pack analysis to statistically investigate the process control. Individual control chart (I chart), moving range chart, capability histogram, values of all observations, normal probability plot and capability plot are summarized in Figure 15 for uncoated and micro-ta-C, ta-C:Cr and ta-C:Ti coated drill bits.
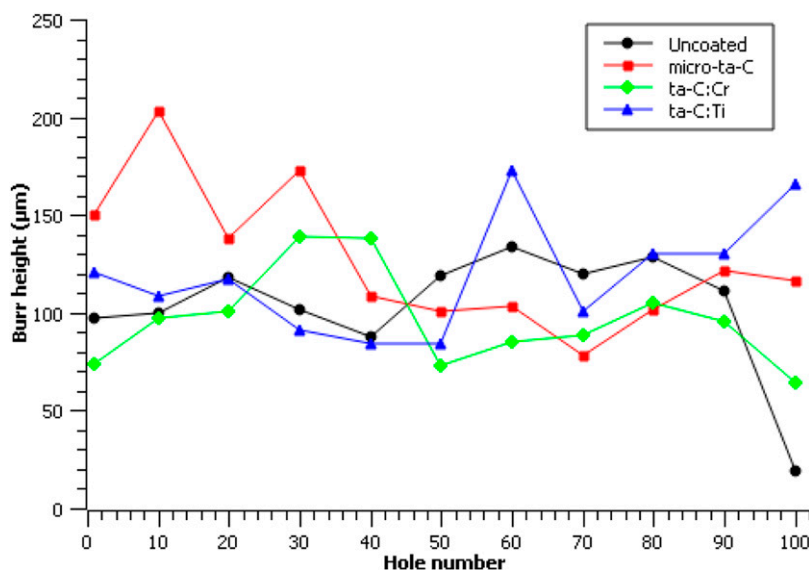

Figure 14. Evolution of maximum burr height as a function of the number of holes drilled by uncoated and coated tools.

Figure 15. Process capability six pack report for the burr height of the holes drilled by (a) uncoated, (b) micro-ta-C coated, (c) ta-C:Cr coated and, (d) ta-C:Ti coated tool in Al7075-T6.

Figure 15. Continued.

First, the analysis of the results presented in I-charts shows that the drilling process is under control for the uncoated and coated tools of this study since all the points are between the control limits (except for the 100th drilled hole produced by uncoated tool (observation 11 in Figure 15(a))). The mean values of H_{bmax} obtained with all the drill bits tested in this study on the overall of the hundred drilled-holes are under the accepted limit. Although all the cutting tools of this study meet industrial requirements of a maximum burr height of 150 µm, it can be noted that ta-C: Cr coated drill bit allows getting the best performance ($\bar{x}$ = 96.4 µm in Figure 15(c)) after the single-shot drilling process.

As shown in Figure 15(a), the PPM of 67700.83 suggests that the actual number of nonconforming parts are considerably low when drilling multi-materials stack using uncoated tool. Although an approximately straight line can be seen in the usual probability plot, it does not fall along the fitted line that is positioned between the confidence bounds. Because the *p*-value (0.012) is less than 0.05, the data does not follow a normal distribution. The high Anderson-Darling statistic value (AD = 0.928) indicates that the data does not closely match the distribution. Despite obtaining C_p values of 1.23 and C_{pk} values of 0.77, they are still below the industry norm, necessitating process modification. Unequal P_{pk} and P_p values (0.50 and 0.80 respectively) proves the process is not centered between the specification limits, and as can be seen from the histogram it is spread more towards the upper specification limit and one point fall extremely outside the lower specification limit. Unequal values of P_{pk} and C_{pk} obtained also shows that the process is not in statistical control.

When considering the burr formation generated by micro-ta-C and ta-C:Ti coated tools (Figure 15(b) and 15(d) respectively), the values of PPM calculated for these two coating types (263376.59 and 146842.57 respectively) suggest that the actual number of nonconforming parts are considerably high. Also, the points don't form an approximately straight line but fall along the fitted line that is located between the confidence bounds in the normal probability plot proves that the data are considerably good. It can also be accepted that the data adheres to normal distribution because the *p*-values are greater than 0.05 (0.247 and 0.401 respectively). The comparatively low Anderson-Darling (0.432 and 0.351 respectively) statistic values show how well the data follow this particular distribution. Though comparatively C_p values around one are obtained (0.93 and 1.01 respectively), these values are smaller than 1.33, thus indicates the process needs to be improved. Unequal P_{pk} and P_p values show that the process is not centered between the specification limits, and as can be seen from the histogram it is spread more towards the upper specification limit. However, the obtention of similar values of P_{pk} and C_{pk} shows that the process is in statistical control.

As depicted in Figure 15(c), the number of non-conforming pieces in terms of burr generation produced when drilling CFRP/Al7075-T6 stack with ta-C:Cr coated tool is the lowest (13886.85) compared to other drill bits tested in this study. Also, the normal probability plot shows that points form an approximately straight line and fall along the fitted line that is located between the confidence bounds and proves the good fit of the data. It can be believed that the data adheres to normal distribution because the *p*-value equals 0.263, which is greater than 0.05. Moreover, the small value of 0.422 in the Anderson-Darling (AD) statistic shows how well the data follow this particular distribution. A higher C_p value (1.38) which is greater than 1.33 shows the process is under good tolerance. Unequal P_{pk} and P_p values (0.73 and 1.03) show that the process is not centered between the specification limits as can also be seen from the capability histogram. Approximately equal values of P_{pk} (0.73) and C_{pk} (0.99) show that the process is in statistical control.

Conclusions

Characterization of coatings showed that the ta-C:Cr coated tool exhibited the lowest coefficient of friction (0.05), while the micro-ta-C coated tool had the highest hardness (26.78 GPa) and bond strength (500 mN). These findings are essential for determining tool usage based on the maximum generated thrust force, temperature etc. And hole quality based on hole edge analysis.

For almost all the holes drilled by micro-ta-C coated tools, the CFRP exit delamination factor was below 1.206, which is the industrial tolerance, for a hole whose diameter is 4.85 mm. However, according to the process capability six pack analysis, the delamination produced by micro-ta-C coated tool also needs to be further controlled to improve the statistical control of the process. Moreover, it was found that the exit delamination decreases as the hardness of the tool and bond strength of the coating increase. On the other hand, uncoated and ta-C:Cr coated tools produced more than half of the parts out of specified limits since they produced a negative C_{pk} and P_{pk} values.

All the tools produced uniform burr in terms of burr height formation. Ta-C:Cr coated tools produced a better maximum burr height, which remained less than 150 µm throughout the operation. When the COF between the workpiece and tool reduced, the exit burr height was also decreased. The process capability six pack analysis also confirmed that the process using ta-C:Cr coated tool in burr height formation was under statistical control since the C_p value of 1.38 and C_{pk} value of 0.99 are good enough for industrial tolerance.

Different coatings will enhance different properties according to their tribological characters. Therefore, choosing the right coating is a greater way to enhance the quality of the drilled holes in order to boost the output and lower the rejection rate. According to the current study, ta-C coated drill shows better properties considering experimental and statistical results. Further analysis on hole integrity performance indicators such as stack up diameter error, hole circularity and hole surface roughness may be useful in determining the interaction of dopant layer added coatings on single-shot drilling of CFRP/Al7075-T6 panels.

Author contributions

J. Joy Mathavan and M.H. Hassan were involved in conceptualization and methodology; J. Joy Mathavan was involved in data collection, formal analysis, writing—original draft, M.H. Hassan and A.S. Mahmud were involved in funding acquisition, resources and investigation, M.H. Hassan was involved in supervision, and project administration, G. Franz was involved in validation, writing—review, formatting and editing.

Declaration of conflicting interests

The author(s) declared no potential conflicts of interest with respect to the research, authorship, and/or publication of this article.

ORCID iD

Muhammad Hafiz Hassan https://orcid.org/0000-0002-8717-8973

References

1. Rajak DK, Pagar DD, Kumar R, et al. Recent progress of reinforcement materials: a comprehensive overview of composite materials. *J Mater Res Technol* 2019; 8(6): 6354–6374. DOI: 10.1016/j.jmrt.2019.09.068
2. Hocheng H and Tsao CC. The path towards delamination-free drilling of composite materials. *J Mater Process Technol* 2005; 167(2–3): 251–264. DOI: 10.1016/j.jmatprotec.2005.06.039
3. Krishnaraj V, Prabukarthi A, Ramanathan A, et al. Optimization of machining parameters at high speed drilling of carbon fiber reinforced plastic (CFRP) laminates. *Compos B Eng* 2012; 43(4): 1791–1799. DOI: 10.1016/j.compositesb.2012.01.007
4. Feito N, Muñoz-Sánchez A, Díaz-Álvarez A, et al. Multi-objective optimization analysis of cutting parameters when drilling composite materials with special geometry drills. *Compos Struct* 2019; 225: 111187. DOI: 10.1016/j.compstruct.2019.111187
5. Erturk AT, Vatansever F, Yarar S, et al. Machining behavior of multiple layer polymer composite bearing with using different drill bits. *Compos B Eng* 2019; 176: 107318. DOI: 10.1016/j.compositesb.2019.107318
6. Li YX, Jiao J, Zhang ZQ, et al. Research on entrance delamination characteristics and damage suppression strategy in drilling CFRP/Ti6Al4V stacks. *J Manuf Process* 2022; 76: 518–531. DOI: 10.1016/j.jmapro.2022.02.018
7. Xu J, Mkaddem A and El Mansori M. Recent advances in drilling hybrid FRP/Ti composite: A state-of-the-art review. *Compos Struct* 2016; 135: 316–338. DOI: 10.1016/j.compstruct.2015.09.028
8. Ramesh B, Elayaperumal A, Satishkumar S, et al. Drilling of pultruded and liquid composite moulded glass/epoxy thick composites: Experimental and statistical investigation. *Measurement* 2018; 114: 109-121. DOI: 10.1016/j.measurement.2017.09.026
9. Gao T, Li C, Wang Y, et al. Carbon fiber reinforced polymer in drilling: From damage mechanisms to suppression. *Compos Struct* 2022; 286: 115232. DOI: 10.1016/j.compstruct.2022.115232
10. An Q, Dang J, Li J, et al. Investigation on the cutting responses of CFRP/Ti stacks: With special emphasis on the effects of drilling sequences. *Compos Struct* 2020; 253: 112794. DOI: 10.1016/j.compstruct.2020.112794
11. Fan L and Wang D. Study on delamination inhibition and chip breakage mechanism in drilling metal laminated materials with double cone drill. *J Manuf Process* 2021; 64: 81–94. DOI: 10.1016/j.jmapro.2021.01.014
12. Shyha IS, Aspinwall DK, Soo SL, et al. Drill geometry and operating effects when cutting small diameter holes in CFRP. *Int J Mach Tool Manufact* 2009; 49(12–13): 1008–1014. DOI: 10.1016/j.ijmachtools.2009.05.009
13. Pawar OA, Gaikhe YS, Tewari A, et al. Analysis of hole quality in drilling GLARE fiber metal laminates. *Compos Struct* 2015; 123: 350–365. DOI: 10.1016/j.compstruct.2014.12.056
14. Zhang L, Liu Z, Tian W, et al. Experimental studies on the performance of different structure tools in drilling CFRP/Al alloy stacks. *Int J Adv Des Manuf Technol* 2015; 81: 241–251. DOI: 10.1007/s00170-015-6955-z
15. Gillespie LK. Deburring precision miniature parts. *Precis Eng* 1979; 1(4): 189–198. DOI: 10.1016/0141-6359(79)90099-0

16. Sui S, Song G, Sun C, et al. Experimental investigation on the performance of novel double cone integrated tool in one-shot drilling of metal stacks *Int J Adv Des Manuf Technol* 2020; 109: 523–534. DOI: 10.1007/s00170-020-05474-9

17. Rivero A, Aramendi G, Herranz S, et al. An experimental investigation of the effect of coatings and cutting parameters on the dry drilling performance of aluminium alloys. *Int J Adv Des Manuf Technol* 2006; 28: 1–11. DOI: 10.1007/s00170-004-2349-3

18. Kim D, Sturtevant C and Ramulu M. Usage of PCD tool in drilling of titanium/graphite hybrid composite laminate. *Int J Mach Mach Mater* 2013; 13(2–3): 276–288. DOI: 10.1504/IJMMM.2013.053228

19. Gao G, Xia Z, Yuan Z, et al. Influence of longitudinal-torsional ultrasonic-assisted vibration on micro-hole drilling Ti-6Al-4V. *Chin J Aeronaut* 2021; 34(9): 247–260. DOI: 10.1016/j.cja.2020.06.012

20. Fiaschi G, Rota A, Ballestrazzi A, et al. A chemical, mechanical, and tribological analysis of DLC coatings deposited by magnetron sputtering. *Lubricants* 2019, 7(4): 38. https://10.3390/lubricants7040038

21. Aisenberg S and Chabot RW. Physics of ion plating and ion beam deposition. *J Vac Sci Technol* 1973; 10: 104–107. DOI: 10.1116/1.1317915

22. Rajak DK, Kumar A, Behera A, et al. Diamond-like carbon (DLC) coatings: classification, properties, and applications, *Appl Sci.* 2021; 11(10): 4445. DOI: 10.3390/app11104445

23. Guo Y, Guo P, Sun L, et al. Tribological properties of Ti-doped diamond-like carbon coatings under dry friction and PAO oil lubrication. *Surf Interface Anal* 2019; 51(3): 361–370. DOI: 10.1002/sia.6588

24. Wang Y, Wang Y, Kang J, et al. Tribological properties of Ti-doped diamond-like carbon coatings under boundary lubrication with ZDDP. *J Tribol* 2021; 143(9): 091901. DOI: 10.1115/1.4049373

25. Outka DA, Hsu WL, Philips K, et al. Compilation of diamond-like carbon properties for barriers and hard coatings. *Sandia National Labs.* 1994. DOI: 10.2172/10151476

26. Murakawa M and Watanabe S. The possibility of coating cubic BN films on various substrates. *Metallurgical Coatings and Thin Films 1990* 1990; 43(1): 145–153. DOI: 10.1016/0257-8972(90)90069-O

27. Franz G, Vantomme P and Hassan MH. A review on drilling of multilayer fiber-reinforced polymer composites and aluminum stacks: optimization of strategies for improving the drilling performance of aerospace assemblies. *Fibers* 2022; 10(9): 78. DOI: 10.3390/fib10090078

28. Hassan MH, Abdullah J and Franz G. Multi-objective optimization in single-shot drilling of CFRP/Al stacks using customized twist drill. *Materials* 2022; 15(5): 1981. DOI: 10.3390/ma15051981

29. Joy Mathavan J, Hassan MH, Xu J, et al. Hole quality observation in single-shot drilling of CFRP/Al7075-T6 composite metal stacks using customized twist drill

30. design. *Journal of Composites Science* 2022; 6(12): 378. DOI: 10.3390/jcs6120378

30. Cheng H, Zhang K, Wang N, et al. A novel six-state cutting force model for drilling-countersinking machining process of CFRP-Al stacks. *Int J Adv Des Manuf Technol* 2017; 89: 2063–2076. DOI: 10.1007/s00170-016-9236-6

31. Davim J and Reis P. Study of delamination in drilling carbon fiber reinforced plastics (CFRP) using design experiments. *Compos Struct* 2003; 59(4): 481–487. DOI: 10.1016/S0263-8223(02)00257-X

32. Gaugel S, Sripathy P, Haeger A, et al. A comparative study on tool wear and laminate damage in drilling of carbon-fiber reinforced polymers (CFRP). *Compos Struct* 2016; 155: 173–183. DOI: 10.1016/j.compstruct.2016.08.004

33. Khashaba UA. Delamination in drilling GFR-thermoset composites. *Compos Struct* 2004; 63(3–4): 313–327. DOI: 10.1016/S0263-8223(03)00180-6

34. Tsao CC and Hocheng H. Taguchi analysis of delamination associated with various drill bits in drilling of composite material. *Int J Mach Tool Manufact* 2004; 44(10): 1085–1090. DOI: 10.1016/j.ijmachtools.2004.02.019

35. Chen WC. Some experimental investigations in the drilling of carbon fiber-reinforced plastic (CFRP) composite laminates. *Int J Mach Tool Manufact* 1997; 37(8): 1097–1108. DOI: 10.1016/S0890-6955(96)00095-8

36. Xu J, An Q, Cai X, et al. Drilling machinability evaluation on new developed high-strength T800S/250F CFRP laminates. *Int J Precis Eng Manuf* 2013; 14: 1687–1696. DOI: 10.1007/s12541-013-0252-2

37. Coromant S. *Users guide - machining carbon fibre materials*. Sandviken: Sandvik coromant, 2010.

38. Dornfeld D and Min S. A review of burr formation in machining. In: Aurich JC and Dornfeld D, editors. *Burrs - analysis, control and removal*. Berlin: Springer, 2010. p. 3–11. DOI: 10.1007/978-3-642-00568-8_1

39. Kurfess TR. *Precision manufacturing, the mechanical systems design handbook: modeling, measurement, and control*. 2017. DOI: 10.1201/9781420036749

40. Franke Burr FV In: CIRP Encyclopedia of Production Engineering, (eds) *CIRP Encyclopedia of Production Engineering*. Berlin: Springer, 2018. p. 1–4. DOI: 10.1007/978-3-642-35950-7_6393-4

41. Cho SJ, Lee KR, Eun KY, et al. Determination of elastic modulus and Poisson's ratio of diamond-like carbon films. *Thin Solid Films* 1999; 341(1–2): 207–210. DOI: 10.1016/S0040-6090(98)01512-0

42. Oliver WC and Pharr GM. An improved technique for determining hardness and elastic modulus using load and displacement sensing indentation experiments. *J Mater Res* 1992; 7: 1564–1583. DOI: 10.1557/JMR.1992.1564

43. Savvides N and Window B. Diamondlike amorphous carbon films prepared by magnetron sputtering of graphite. *J Vac Sci Technol A: Vacuum, Surfaces, and Films* 1985; 3(6): 2386–2390. DOI: 10.1116/1.572887

44. Voevodin AA and Donley MS. Preparation of amorphous diamond-like carbon by pulsed laser deposition: a critical review. *Surf Coating Technol* 1996; 82(3): 199–213. DOI: 10. 1016/0257-8972(95)02734-3

45. Zhang S, Bui XL, Zeng XT, et al. Towards high adherent and tough a-C coatings. *Thin Solid Films* 2005; 482(1–2): 138–144. DOI: 10.1016/j.tsf.2004.11.165

46. Zhong B, Zou F, An Q, et al. Experimental study on drilling process of a newly developed CFRP/Al/CFRP co-cured material. *J Manuf Process* 2022; 75: 476–484. DOI: 10. 1016/j.jmapro.2021.12.062

47. D'Orazio A, El Mehtedi M, Forcellese A, et al. Tool wear and hole quality in drilling of CFRP/AA7075 stacks with DLC and nanocomposite TiAlN coated tools. *J Manuf Process* 2017; 30: 582–592. DOI: 10.1016/j.jmapro.2017.10.019

48. Sridhar AK, Bolar G and Padmaraj NH. Comprehensive experimental investigation on drilling multi-material carbon fiber reinforced aluminum laminates. *J King Saud Univ Sci* 2021; 34(7): 391–401. DOI: 10.1016/j.jksues.2021.11.004

49. Min S, Kim J and Dornfeld DA. Development of a drilling burr control chart for low alloy steel, AISI 4118. *J Mater Process Technol* 2001; 113(1–3): 4–9. DOI: 10.1016/S0924-0136(01)00589-1

50. Hazarika M and Dixit US. *Setup planning for machining*. Berlin: Springer International Publishing, 2014.

51. Niknam SA, Zedan Y and Songmene V. Machining burrs formation & deburring of aluminium alloys. In: Monteiro WA, (eds). *Light metal alloys applications*. London, UK: IntechOpen, 2014. https://www.intechopen.com/chapters/46639

52. Bahçe E and Özdemir B. Investigation of the burr formation during the drilling of free-form surfaces in al 7075 alloy. *J Mater Res Technol* 2019; 8(5): 4198–4208. DOI: 10.1016/j. jmrt.2019.07.028

53. Köklü U. Influence of the process parameters and the mechanical properties of aluminum alloys on the burr height and the surface roughness in dry drilling. *Materials and Tehnologies* 2012; 46(2): 103–108.

54. Kundu S, Das S and Saha PP. Optimization of drilling parameters to minimize burr by providing back-up support on aluminium alloy. *Procedia Eng* 2014; 97: 230–240. DOI: 10. 1016/j.proeng.2014.12.246

55. Dahnel AN, Fauzi MH, Raof NA, et al. Tool wear and burr formation during drilling of aluminum alloy 7075 in dry and with cutting fluid. *Mater Today Proc* 2022; 59: 808–813. DOI: 10.1016/j.matpr.2022.01.110

56. Hassan MH, Abdullah J, Mahmud AS, et al. Burr height as quality indicator in single shot drilling of stacked CFRP/ Aluminium composite. *Key Eng Mater* 2017; 744: 327–331. DOI: 10.4028/www.scientific.net/kem.744.327

57. Hassan MH and Razali MF. Comparison of coated and uncoated drill bit on the drilling quality of CFRP/AL7075-T6 stacked materials. In Proceedings of Mechanical Engineering Research Day, 16 December 2020. Universiti Teknikal Melaka 2020. pp. 336–338.

58. Kuo CL, Soo SL, Aspinwall DK, et al. Development of single step drilling technology for multilayer metallic-composite stacks using uncoated and PVD coated carbide tools. *J Manuf Process* 2018; 31: 286–300. DOI: 10.1016/j.jmapro.2017.11.026